

Article

Iterative Trajectory Planning and Resource Allocation for UAV-Assisted Emergency Communication with User Dynamics

Zhilan Zhang¹, Yufeng Wang^{2,*}, Yizhe Luo³, Hang Zhang¹, Xiaorong Zhang¹ and Wenrui Ding²

¹ School of Electronics and Information Engineering, Beihang University, Beijing 100083, China; zzl1223@buaa.edu.cn (Z.Z.); zhangh102@buaa.edu.cn (H.Z.); zhangxiaorong@buaa.edu.cn (X.Z.)

² Institute of Unmanned System, Beihang University, Beijing 100083, China; ding@buaa.edu.cn

³ School of Computer and Artificial Intelligence, Zhengzhou University, Zhengzhou 450001, China; luoyizhe@zzu.edu.cn

* Correspondence: wyfeng@buaa.edu.cn

Abstract: The demand for air-to-ground communication has surged in recent years, underscoring the significance of unmanned aerial vehicles (UAVs) in enhancing mobile communication, particularly in emergency scenarios due to their deployment efficiency and flexibility. In situations such as emergency cases, UAVs can function as efficient temporary aerial base stations and enhance communication quality in instances where terrestrial base stations are incapacitated. Trajectory planning and resource allocation of UAVs continue to be vital techniques, while a relatively limited number of algorithms account for the dynamics of ground users. This paper focuses on emergency communication scenarios such as earthquakes, proposing an innovative path planning and resource allocation algorithm. The algorithm leverages a multi-stage subtask iteration approach, inspired by the block coordinate descent technique, to address the challenges presented in such critical environments. In this study, we establish an air-to-ground communication model, subsequently devising a strategy for user dynamics. This is followed by the introduction of a joint scheduling process for path and resource allocation, named ISATR (iterative scheduling algorithm of trajectory and resource). This process encompasses highly interdependent decision variables, such as location, bandwidth, and power resources. For mobile ground users, we employ the cellular automata (CA) method to forecast the evacuation trajectory. This algorithm successfully maintains data communication in the emergency-stricken area and enhances the communication quality through bandwidth division and power control which varies with time. The effectiveness of our algorithm is validated by evaluating the average throughput with different parameters in various simulation conditions and by using several heuristic methods as a contrast.

Keywords: unmanned aerial vehicles; resource allocation; trajectory planning; iterative scheduling; cellular automata



Citation: Zhang, Z.; Wang, Y.; Luo, Y.; Zhang, H.; Zhang, X.; Ding, W. Iterative Trajectory Planning and Resource Allocation for UAV-Assisted Emergency Communication with User Dynamics. *Drones* **2024**, *8*, 149. <https://doi.org/10.3390/drones8040149>

Academic Editor: Emmanouel T. Michailidis

Received: 13 March 2024

Revised: 7 April 2024

Accepted: 9 April 2024

Published: 11 April 2024



Copyright: © 2024 by the authors. Licensee MDPI, Basel, Switzerland. This article is an open access article distributed under the terms and conditions of the Creative Commons Attribution (CC BY) license (<https://creativecommons.org/licenses/by/4.0/>).

1. Introduction

UAV-assisted mobile communication takes the role of an efficient technology that uses unmanned aerial vehicles (UAVs) as communication nodes in wireless networks, with UAVs performing as aerial base stations, communication relays, and data connection stations. In research on B5G/6G communication, UAVs have already been widely applied [1]. They can provide enhanced coverage, capacity, and connectivity for applications in various communication scenarios, such as surveillance management [2], smart agriculture [3], and aerial delivery [4]. Drone-assisted IoT (the Internet of Things) systems are also called IoD (Internet of Drones) [5]. The authors in [6] have demonstrated the data collection ability of drones, which is also applied in emergency [7] or MEC cases [8]. More than a data transmitting node, a UAV can also serve as a cloud computation center with limited ground processing capability [9]. In other applications, UAVs provide sensing [10], target search [11], and healthcare supply service [12,13] based on their mobility.

In recent years, the integration of UAVs into emergency communication systems has caught significant attention due to their ability to overcome limitations in traditional ground base stations [14]. In emergency-stricken cases, disasters such as earthquakes, hurricanes, and wildfires can inflict severe damage on ground communication infrastructure, making them either disabled or inaccessible. Consequently, timely and reliable communication services in such contexts play a vital role in rescue and response. Both civil and military institutions can benefit from UAV-assistance communication. Emergency response agencies like FEMA (Federal Emergency Management Agency) would be interested in leveraging UAVs to enhance communication capabilities during disasters or emergencies, while telecommunication companies could benefit from UAV-assisted communication planning algorithms to improve their capacity for assisting in affected areas. During the 2021 Henan flood, China Mobile dispatched Yilong drones to temporarily restore communication in the disaster area. UAV-assisted mobile communication has several advantages over traditional terrestrial or satellite-based communication systems, such as flexibility, mobility, scalability, ease of deployment, and low cost, therefore they can match the requirements needed in emergency communication cases.

However, the field also encounters many challenges, especially in intricate problems. In UAV deployment, costs of moving and energy consumption need to be considered, which provide constraints on assistance quality optimization. In problems of trajectory planning or routing, the communication environment changes rapidly, resulting in imperfect channel state information. Coordination, security, and power management also matter in related problems, making the algorithm design rather complicated [9]. Generally speaking, research on UAV-assisted communication mainly involves two aspects: one is the establishment of an air-ground communication model, and the other is the design and optimization of drone scheduling algorithms.

1.1. Related Works

Differing from conventional ground-based communication, air-to-ground (A2G) communication is subject to the influence of altitude differentials, thus presenting a more complex and dynamic model of the environment [15]. In recent years, many researchers have focused on the design of evaluating indicators, along with communication models in both general and certain environments [16] for air-to-ground channels. To assess the effectiveness and robustness of UAV-assisted networks, various metrics have been proposed for A2G networks. The authors in [17] considered energy efficiency, while [18] considered throughput. In [19], the average completion time of subtasks was applied for assessment. Other evaluating factors include the arrival rate, spectral efficiency, and channel capacity, while factors such as time delay, coverage [20], and outage probability also affect A2G networks.

Communication parameters of A2G channels differ in typical scenes involving different environments such as urban, dense urban, suburban, etc. In [21], researchers developed the A2G path loss model in the urban environment, while [22] focused on multilink channel model analysis at 2.4 and 5.9 GHz, both in low altitude circumstance. For aerial sensor networks, [23] introduced a realistic channel model leveraging cooperative UAVs in order to reach maximum spatial exploration efficiency. In [24], the statistical characteristics of the airframe shadowing loss were further analyzed. In [25], the authors gave a spatially and temporally correlated A2G channel model in cellular-connected UAV swarms, as well as a design for performance analysis. Ref. [26] considered atmospheric refractivity and precipitation, and they obtained path loss along the range and altitude. Moreover, [27] proposed a clustering method to analyze time-varying channels.

Blessed with auto-mobility and self-decision ability, UAVs can usually perform as aerial base stations in emergency cases when ground base stations are blocked. To execute communication assistance missions, researchers need to design trajectory planning and resource allocation algorithms for UAVs' scheduling. In the field of UAV trajectory planning, researchers have proposed various algorithms and methods to address path-planning

problems in different environments. Heuristic-based methods employ heuristic algorithms such as genetic algorithms, simulated annealing, etc., to find optimal paths. Heuristic-based methods are often suitable for complex environments but may exhibit lower efficiency for large-scale problems. Ref. [28] introduced a 3-D path planning method improved from ant colony optimization, and Ref. [29] searched the UAV configuration space with a modified Mayfly algorithm. For collision avoidance, the slime mold algorithm (SMA) performs well with a design preventing it from local optimization points [30]. Inspired by a genetic algorithm, [31] proposed the ANSGA-III method with enhanced planning ability in complex environments. Graph theory-based methods model the environment as a graph and use classical graph algorithms to find the shortest or optimal paths, which also tend to perform well in simple environments. Ref. [32] discussed an approach of dynamic coloring for UAV planning in emergency cases, and [33] proposed a 3-D deployment method based on Dijkstra's algorithm, with UAV playing both as an aerial base station and relays. The idea of TSP (Traveling Salesman Problem) was applied in [18] with classified stressed regions, while [34] combined graph theory and convex optimization. Moreover, recent years have witnessed remarkable advancements in path planning facilitated by deep learning methodologies. Convolutional neural networks (CNNs) and recurrent neural networks (RNNs) have been employed to predict flight trajectories and have shown impressive performance in complex environments. Deep reinforcement learning (DRL) techniques have also been harnessed for this purpose, further contributing to enhanced performance. The trajectory planning method varies with the environment. Path planning for UAVs in windy environments was proposed in [35], with simulated moving targets for UAVs to pursue. Ref. [36] took advantage of the traditional collision avoidance method and DRL method, resulting in long trajectory planning with unknown obstacles. In [37], UAVs serve in a warehouse for stock inventory, updating real-time paths with image recording.

Resource allocation constitutes another critical aspect of ensuring UAV assistance. The efficiency of UAVs is often limited by their battery life, prompting research into spectrum resource allocation and efficient energy management [38], including task scheduling and dynamic recharging strategies. Given that the resource allocation problem is NP-hard, researchers strive for sub-optimal solutions using methods from convex optimization, machine learning, etc. Zhang et al., in [39], proposed a safe-DQN method to optimize UAV trajectories, considering constraints such as user equipment (UE) energy limits and obstacles in emergency scenarios. Furthermore, for target assignment in multi-object scenes, multi-agent reinforcement learning (MARL) has been demonstrated to be effective, as shown in [40].

In the context of an evacuation, the trajectory of moving ground users requires statistical data or simulation for accurate consideration [41]. Since the moving behavior of users varies with the environment, cellular automata can be employed to adjust their trajectories. Cellular automata model the map as a two-dimensional grid space and assign different values to different grids to represent users, obstacles, exits, etc. Therefore, the state transition of certain grids can be predicted according to the states of their neighboring grids. Ref. [42] utilized cellular automata in forest fire spread prediction, specified influencing factors to adjust cell state and cell transition rules, and gave a 3D visualization for the fire spread model. In [43], cellular automata and the ant colony algorithm were used to optimize the evacuation model, which is applicable in emergency scenarios.

1.2. Our Contributions

To address the challenges in the communication of emergency cases, we propose an iterative scheduling algorithm for trajectory and resource (ISATR) for path planning and limited resource allocation in a UAV-assisted emergency communication network. In addition to commonly discussed variables, we consider the dynamics of ground users and present a comprehensive approach using a quasi-convex method to optimize UAV path, power, and bandwidth allocation across different time slots. This approach spans

dimensions of time, space, spectrum, and energy; therefore, it can provide a rather accurate and comprehensive plan. The main contributions of this paper are summarized as follows:

1. UAV-assisted communication model with the dynamic environment. For emergency cases, few researchers test their algorithm with dynamic users. We have established an A2G communication model with moving ground users, where the energy consumption and assistance communication quality are jointly optimized.
2. Dynamic bandwidth allocation. For resource allocation in UAV-assisted communication, few researchers focus on bandwidth, due to its high complexity. Our work tackles dynamic bandwidth allocation, providing an algorithm for real UAV planning.
3. Designed iterative algorithm. For the NP-hard optimization problem of UAV planning in emergency communication, we leverage the idea of subtask iterative algorithm and work out an effective iterative scheduling algorithm of trajectory and resource.
4. Simulation analysis. Experiments are implemented to evaluate the effectiveness of the proposed optimization algorithm, which achieves obvious performance compared with non-optimized and several other methods and can maintain the performance in different environments.

Benefiting from its high accuracy, ISATR can serve as a necessary baseline in case of emergency communication situations, applied for a pre-planning scheme derived before emergency strikes.

This paper is organized as follows:

- The A2G communication model, user moving strategy, and mathematical optimization model are established in Section 2.
- The iterative scheduling algorithm for trajectory and resource (ISATR) is elaborated on in Section 3.
- In Section 4, the results and performance are discussed, with comparisons in different environments.
- Section 5 concludes the paper.

2. Modeling of UAV-Assisted Communication

2.1. UAV Air-to-Ground Channel Model

In dense urban environments, communication is primarily supported by ground-based stations serving mobile users distributed across cellular networks. However, during certain emergencies such as earthquakes, urban communication infrastructure may fail. When the ground-based station in the earthquake-stricken area malfunctions, it results in the loss of signal coverage within the community. This disruption complicates communication for ground users, leading to panic and impeding emergency relief efforts. Therefore, unmanned aerial vehicles (UAVs) are introduced as temporary aerial base stations to provide communication services in emergency scenarios. In this section, we present the basic model of UAV-assisted A2G communication.

When the ground base station malfunctions, the UAV can be utilized as an aerial base station to serve urgent communication. Before establishing a UAV-assisted emergency communication model, it is necessary to discuss the air-to-ground channel. In A2G communication, there are LoS (line of sight) paths and NLoS (not line of sight) paths, in which the NLoS is obstructed by obvious obstacles. While A2G communication can enjoy LoS channel in common cases, NLoS channel occurs when obstacles exist. As Figure 1 demonstrates, urban architecture and natural landscape both perform as obstacles in UAV-assisted communication. The occurrence probability for LoS/NLoS channel differs according to the location of UAV and the density of obstacles.

It can be seen that the ratio of LoS and NLoS path varies with the height of UAV. Therefore, a probabilistic LoS/NLoS channel model is applied [21] with parameter p_{LoS} to denote the occurrence probability of LoS channel and p_{NLoS} for that in NLoS channel. In

consideration of varied environmental factors, p_{LoS} and p_{NLoS} for a single A2G link can be calculated by Equations (1) and (2).

$$p_{LoS} = \alpha \left(\frac{180\theta}{\pi} - 15 \right)^\gamma, \tag{1}$$

$$p_{NLoS} = 1 - \alpha \left(\frac{180\theta}{\pi} - 15 \right)^\gamma, \tag{2}$$

in which θ refers to the elevation angle between each user equipment and UAV, reflecting the impact of UAV height and position on the link. Parameters α and γ are influenced by environmental characteristics at the same time.

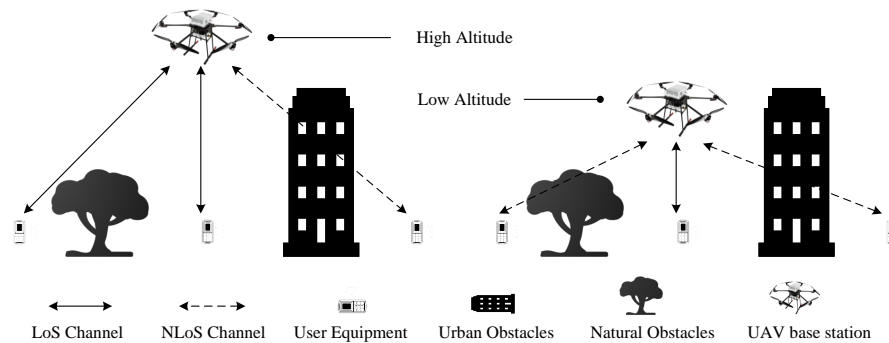


Figure 1. LoS/NLoS A2G channels in UAV-assisted communication. The model consists of a UAV aerial base station, ground user equipment, urban obstacles, and natural obstacles, which can influence LoS probability and then determine the A2G channel.

In the discussed earthquake-stricken cellular cells, mobile users evacuate from buildings and move toward certain exits. The ground base station breaks, interrupting communication. To plan a UAV for urgent communication, we need to model the environment of the cell, and then adjust the UAV’s resources and location to maximize communication quality.

As Figure 2 displays, the path of a UAV can be planned according to ground users’ evacuation trajectory in order to enhance communication quality and increase coverage.

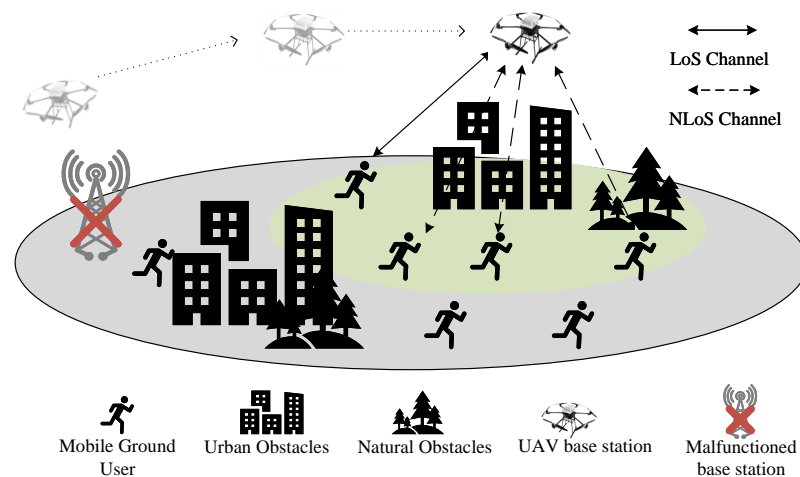


Figure 2. UAV-assisted emergency communication with malfunctioned ground base station and moving users. The model considers obstacles that impact both the trajectory of users and the signal transmission with the UAV base station, and our research is dedicated to the scheduling of UAV trajectory and resources to optimize the efficiency of communication during the evacuation.

The LoS path of UAV is obstructed by several obstacles, including compound buildings and greenery such as trees. Buildings are also regarded as obstacles for mobile users to evacuate from. Moreover, at each communication timeslot, transmission power and spectrum division of the UAV are determined.

As the proposed problem mainly focuses on the path planning and resource allocation algorithm of the UAV base station, a number of assumptions are introduced to simplify the model with no influence on algorithm construction. The UAV and valid moving ground users are constrained in the area of earthquake-stricken cells, which means one user turns invalid as soon as he/she runs out of the exit. When optimizing the trajectory, the height of UAV is fixed in each experiment. The FDMA (frequency division multiple access) technique is applied; thus, there is no interference between ground users and between ground users to drones.

To build up this UAV-assisted communication model, specifically defined parameters, formulas, and functions are introduced as follows. Briefly speaking, air-to-ground communication quality is used as an evaluation index and expressed in terms of system throughput.

Communication throughput depends on the arrival rate of bi-directional links. Therefore, transmission power of uplink and downlink channels in A2G communication can be calculated, followed by the corresponding SINR (Signal to Interference plus Noise Ratio). P_{ug} denotes received power at ground users in downlink communication, with P_{gu} defined for received power at UAV in uplink mode. Taking the link parameter into consideration, $P(u, g_j)$ describes transmission power between link j , in which u refers to UAV and g_j refers to j^{th} ground user. The probabilistic LoS/NLoS space power propagation model is clarified in (3) and (4), which defines transmission power P , received gain G , euclidean distance d , and environmental loss parameter k_0 . P_{LoS} and P_{NLoS} refer to the occurrence possibility of LoS and NLoS channel, while ϕ_{LoS} and ϕ_{NLoS} refer to the corresponding shadow parameters.

$$P_{ug}(u, g_j) = \frac{P_u G(d_j)}{(k_0 d_{ij})^n (p_{LoS} \phi_{LoS} + p_{NLoS} \phi_{NLoS})}. \quad (3)$$

$$P_{gu}(u, g_j) = \frac{P_g G_0}{(k_0 d_{ij})^n (p_{LoS} \phi_{LoS} + p_{NLoS} \phi_{NLoS})}. \quad (4)$$

$$SINR_{ug} = \frac{P_{ug}(u_i, e_j)}{\sigma^2}, SINR_{gu} = \frac{P_{gu}(u_i, e_j)}{\sigma^2}. \quad (5)$$

Finally, the throughput is calculated through Shannon's law as follows, as the considered communication occurs in the channel with AWGN (Additive White Gaussian Noise).

$$C = B \times \log_2(1 + SINR). \quad (6)$$

2.2. User Trajectory Prediction Model

Before conducting optimization for UAV path planning and resource allocation, it is essential to define the ground users' moving trajectories as the initial input data for optimizing UAV strategies, as we consider user dynamics. In this context, we introduce the cellular automata (CA) method as a means to simulate and predict the users' moving trajectories.

Cellular automata (CA) is a discrete grid-based dynamic model that encompasses discrete representations of time, space, and state variables. Notably, it exhibits a localized spatial interaction and temporal causality, enabling it to simulate the spatiotemporal evolution process of intricate systems. CA methods have been found with extensive applications, including fire spread simulations and other domains. Due to its capability to achieve a balance between accuracy and efficiency, CA is also well-suited for simulating evacuation scenarios.

The CA model is kind of a multi-dimensional dynamic programming method to some degree, as shown in Figure 3. Grids represent states at each location and are influenced

by neighbor grids based on certain transition probability matrices. With the idea of the CA model, the method for predicting users' trajectories is then derived. To simplify the evacuation model, we suppose all the mobile users in the earthquake-stricken compound have already left their residential buildings and, therefore, are initially located within so-called valid areas. Once a user successfully escapes from the evacuation exit, his or her location becomes invalid and is no longer considered in the calculation of the overall communication throughput.

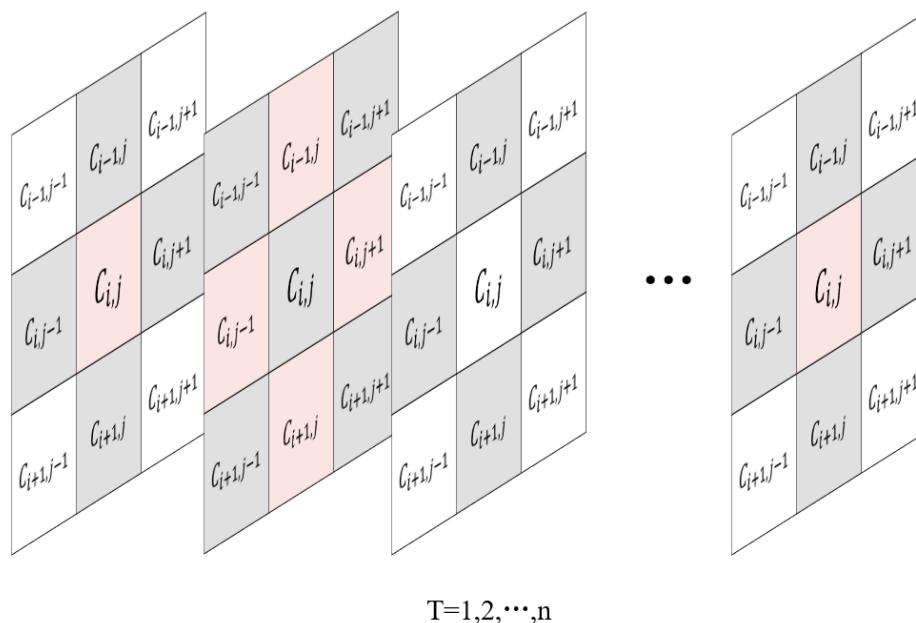


Figure 3. Cellular automata schemes. States of grids change according to states of neighbors; thus, they can predict data along time sequence with an initial input. CA model is applied to generate the evacuation trajectory data of users.

Considering that the moving ground users are residents of the neighborhood, it is reasonable to assume that they possess knowledge of the map, including the distribution of obstacles and the location of exits. Accordingly, it can be supposed that the moving trajectory of each ground user follows the shortest path from their current location to the evacuation exit.

Suppose there are overall K users placed randomly in the valid area of the cellular zone, with only one exit, while residential buildings play as obstacles in the area. The environment is modeled as a 2-dimensional grid map, and the moving direction of the ground user can be defined in a discrete direction set $D = \{\text{east, south, west, north, northeast, southeast, northwest, southwest}\}$, mapping to numbers 0 to 7.

Mobile users select their moving direction from the direction set D according to the current location, and adjust moving speed regarding current crowd density, namely the influence of neighbor grids. The moving speed affected by the current density of adjacent users is defined in the following equation:

$$v = v_0 / \rho \text{ (m/s)}, \tag{7}$$

in which v_0 refers to the typical moving speed of humans with no obstacles and neighbors. ρ changes with the current number of users in a neighbor range, being an integer no less than 1 m/s. Therefore the state of any grid can be initialized and then transformed into a next state step by step, until reaching convergence.

By this means, after gridding the current map, the evacuation trajectories of users with different initial distributions can be obtained through the CA method, and obtain the data of user positions at each time point. The gridded map is illustrated in Figure 4.

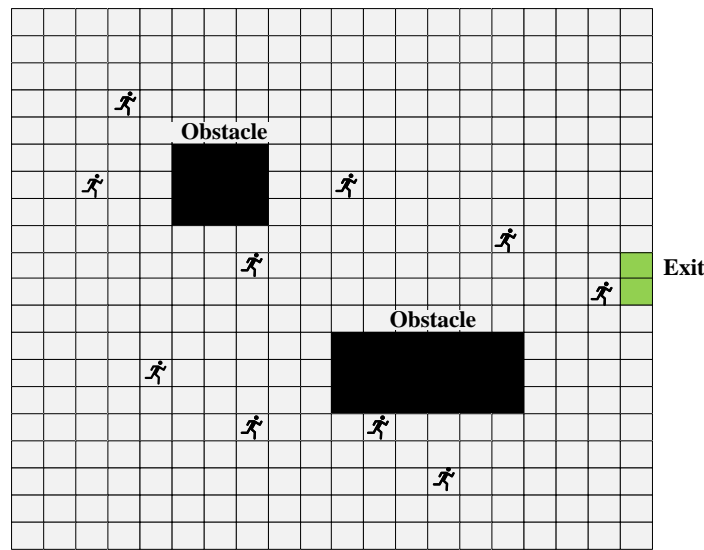


Figure 4. Grid map of valid evacuation area. The area includes obstacles, one exit, and 10 ground users in the simulation. Each grid equals a square area of 1 m × 1 m in actual simulation.

2.3. Optimization Mathematical Model

In the UAV-assisted emergency communication discussed above, we propose the air-to-ground communication model and simulation of the user evacuation trajectory. The optimization mathematical functions are defined in this section, followed by complexity analysis.

The main task is to recover the interrupted service and enhance communication quality; thus, we set the total throughput as the objective function in optimization, as shown in Equation (8). In the planning model with K users and N time slots, user location, bandwidth division, and transmission power are considered decision variables. Both uplink and downlink communication happens, regarding the UAV as the aerial base station.

$$R_{i,n} = \frac{1}{2} \cdot B_n \cdot [\log_2(1 + SINR_{ug}) + \log_2(1 + SINR_{gu})]. \tag{8}$$

Subscript i represents the current moving user and subscript n represents the current time slot. Moreover, design for constraint functions is also necessary. In the above discussions, it can be seen that the objective function consists of the bi-directional arriving rate $R_{i,n}$ at each resource block. On one side, as UAVs have real physical characteristics, the energy, velocity, and power are limited. On the other, the communication resource is also limited, involving maximum bandwidth.

Therefore, the constraint variables are divided into 3 sets, which are $U = [v_n, a_n]$, $B = [B_n]$, and $P = [E_n^C, E_n^F, P_n]$, referring to variables of UAV's location and velocity, variables of bandwidth resource, and variables of energy and power consumption. E_n^C represents communication energy cost at time slot n , and E_n^F refers to flight consumption. To ensure data communication, the lower bound of R_i is also specified. The total optimization functions are shown in Equation (9),

$$\begin{aligned} & \max_{UBP} \sum_n \sum_i R_{i,n} \\ & \text{s.t.} \begin{cases} 0 \leq P_u \leq P_{max} \\ \sum_i^C E_{i,n} + E_n^F \leq E_{max} \\ \sum B_{i,n} \leq B_i \\ v_n \leq v_{max} \\ R_{min} \leq R_i \end{cases} \end{aligned} \tag{9}$$

The complexity of the discussed problem is proved to be NP-hard (non-deterministic polynomial-time hard) in this section, which can reveal the significance and effectiveness of our algorithm.

NP means a problem can not be resolved in polynomial time, and all the NP problems can be reduced to the NP-hard problem. Reduction is a reversible process, which means that the solvers of both problems can be transformed into one. Therefore, any certain problem can be proved NP-hard if it can be reduced to other typical NP-hard problems.

According to the list of proven NPH problems, the bounded knapsack problem (BKP) is a NPH model with a basic optimization model:

$$\begin{aligned} \max \quad & \sum_{i=1}^n v_i x_i \\ \text{s.t.} \quad & \left\{ \sum_{i=1}^n w_i x_i \leq W, \quad x_i \in 0, 1, 2, \dots, c \right. \end{aligned} \quad (10)$$

x_i refers to decision sequence, while w_i stands for weight cost and v_i represents value. Similarly, in our problem, the decision sequence for UAV aims to maximize total throughput with certain v_i factors, and weight constraints are controlled in the communication energy aspect. Thus, our problem can be reduced to a bounded knapsack problem, which indicates the NPH characteristic of our model. Therefore, the joint optimization problem discussed can only achieve an approximate solution, necessitating highly accurate algorithms.

3. Iterative Scheduling Algorithm for Throughput Optimization

To address the multi-objective optimization in the evacuation scenario, two primary stages require deliberation, after the establishment of the communication model outlined in the preceding section. The initial stage involves predicting unknown environmental information, specifically the trajectories of moving ground users. Subsequently, the second stage revolves around formulating an optimization algorithm for UAV to enhance total communication efficiency based on these predictions.

3.1. Algorithm Architecture of ISATR

In the non-linear optimization field, the coordinate descent method differs from the gradient descent method, as it searches for optimal values along all coordinates. The block coordinate descent method adds the problem division stage to the traditional coordinate descent method, which means it performs coordinate descent on several designed sub-problems.

$$\mathbf{x}_i^{(k)} = \arg \min_{\mathbf{x}_i} f(\mathbf{x}_1^{(k)}, \dots, \mathbf{x}_{i-1}^{(k)}, \mathbf{x}_i, \mathbf{x}_{i+1}^{(k-1)}, \dots, \mathbf{x}_n^{(k-1)}). \quad (11)$$

As shown in (11) and Algorithm 1, the block coordinate descent algorithm groups all the variables into several blocks including x_1, x_2, \dots, x_n , and then in each iteration, only the variables in one block are optimized, while the variables in the other blocks remain unchanged. By updating the variables in different blocks alternately, the objective function is finally reduced.

To tackle the throughput optimization problem with high complexity, we designed the ISATR (iterative scheduling algorithm of trajectory and resource) for this solution, inspired by the idea of BCD. The variables are divided into three categories, which are location, transmission power, and bandwidth allocation of UAV at all considered time slots.

The energy cost of flight consumption is calculated in Equation (12), followed by communication cost derived in Equation (13). E^C represents communication energy cost, with normalized emission power P_0 of unit space distance. E^F refers to flight consumption. Other relative variables and abbreviations are listed in Table 1.

$$E^C = \sum_n \sum_i P_0 \Delta T. \quad (12)$$

$$E^F = \sum_n^N mv_n^2. \quad (13)$$

Algorithm 1: Block coordinate descent algorithm

Data: Initial variables in n designed blocks $X = \{x_1^0, x_2^0, \dots, x_n^0\}$
Result: Optimal $\{x_1, x_2, \dots, x_n\}$

```

1  $X \leftarrow X_0$ ;
2 for  $k = 1, 2, \dots$  do
3   for  $i = 1, 2, \dots$  do
4      $x_i^k \leftarrow x_i^k$ , update  $x_i^k$  with other blocks fixed;
5   end
6 end
7 if stopping criteria satisfied then
8   return  $\{x_1^k, x_2^k, \dots, x_n^k\}$ ;
9 end

```

Table 1. Abbreviation definitions.

Variable	Definition
m	Mass of UAV
u_n	UAV location at n th time slot
a_n	Flight direction of UAV at n th time slot
v_n	Flight velocity of UAV at n th time slot
v_{max}	Maximum flight speed of UAV
$e_{i,n}$	i th user's location at n th time slot
$P_{u,n}$	Transmission power of UAV at n th time slot
P_{max}	Upper bound of transmission power
$B_{i,n}$	Bandwidth allocated to i th user at n th time slot
B_i	Total bandwidth for A2G communication at time slot i
$E_{i,n}^C$	UAV communication power consumption with i th user at n th time slot
E_n^F	UAV flight energy consumption in n th time slot
E_{max}	Upper bound of total energy consumption
R_i	Throughput for communication with user i
R	Total throughput of A2G communication

The simulation process terminates when the last moving ground user has left the evacuation exit. Details of the iterative algorithm are clarified in Equation (14), followed by its pseudo-code Algorithm 2, with complexity also discussed.

$$\begin{aligned}
 & \max_{UBP} \sum_n^N \sum_i^K R_{i,n} \\
 & s.t. \begin{cases} 0 \leq P_u \leq P_{max} \\ \sum_i^C E_{i,n} + E_n^F \leq E_{max} \\ \sum B_{i,n} \leq B_i \\ v_n \leq v_{max} \\ R_{min} \leq R_i \end{cases} \quad (14)
 \end{aligned}$$

The complexity of ISATR is also derived. For the block of UAV trajectory planning, the time complexity is $O(NK)$, where N represents the number of time steps and K denotes the number of users. In each time step, the algorithm iterates over each user to calculate the distance between the UAV and each user. This involves a loop nested within the time step loop, resulting in a time complexity proportional to the product of N and K . Moreover, constant-time calculations are performed to determine the signal-to-interference-plus-noise ratio (SINR) and to update the total throughput. Therefore, the time complexity of this

Algorithm 2: ISATR (Iterative Scheduling Algorithm of Trajectory and Resource)

Data: Initial variables in designed blocks $X = \{x_U^0, x_B^0, x_P^0\}$
Result: Optimal sets $\{U, B, P\}$

- 1 $x_U^0 \leftarrow \{u_n\}, u_0 = [0, L/2], u_n = u_{n-1} + [v_0 \cdot \cos a_0, v_0 \cdot \sin a_0];$
- 2 $x_B \leftarrow \{B_i\}, B_i = B/K;$
- 3 $x_P \leftarrow \{P_0\};$
- 4 **for** $t = 1, 2, \dots$ **do**
- 5 **for** $k = 1, 2, \dots, K$ **do**
- 6 **for** $i = 1, 2, \dots, N$ **do**
- 7 $x_B \leftarrow x_B^{t-1}, x_P \leftarrow x_P^{t-1};$
- 8 update $x_U^t(i, k)$ with other blocks fixed;
- 9 $x_U \leftarrow x_U^{t-1}, x_P \leftarrow x_P^{t-1};$
- 10 update $x_B^t(i, k)$ with other blocks fixed;
- 11 $x_U \leftarrow x_U^{t-1}, x_B \leftarrow x_B^{t-1};$
- 12 update $x_P^t(i, k)$ with other blocks fixed;
- 13 **end**
- 14 **end**
- 15 **end**
- 16 **if** stopping criteria satisfied **then**
- 17 return $\{x_U^T, x_B^T, x_P^T\};$
- 18 **end**

block is $O(NK)$. Similar to the UAV positions optimization, the time complexity of the other two blocks is also $O(NK)$.

Therefore, the complexity of our method can be derived as $O(NK)$, in which K represents user number, and N represents time slots, which can be regarded as $O(n^2)$.

3.2. UAV Trajectory Subtask Optimization

The first sub-optimization problem block focuses on UAV path planning, with full knowledge of external information acquired in the previous iteration round, including resource allocation and environmental states. The sum of R_i stands for the objective function, namely the total throughput of the A2G communication links.

$$\begin{aligned}
 \text{Objective} &= \sum R_i \\
 &= \sum B * \log_2(1 + \text{SINR}) \\
 &= \sum B * \log_2\left(1 + \frac{P_{ug}(u_i, e_j)}{\sigma^2}\right).
 \end{aligned} \tag{15}$$

As the UAV location changes, the parameters of the A2G communication channel model and the distance between UAV base station and ground users also change, which can be determined by UAV position and known environmental information. Environmental parameters also depend on the UAV's location, thus influencing the SINR value of communication links. Therefore, when fixing the other two sub-optimization blocks, the objective function can be regarded as a function of the UAV's position vector.

To design the location optimization block, constraints of acceleration and energy limitation are considered, which are performed as unequal constraints.

$$\begin{aligned} & \max_{u_n, v_n} \sum_i^K R_i \\ & \text{s.t.} \quad \begin{cases} \sum_n^N \sum_i E_{i,n}^C + \sum_n E_n^F \leq E_{max} \\ \mathbf{0} \leq u_n \leq [x_{max}, y_{max}] \\ -\pi \leq a_n \leq \pi \\ v_n \leq v_{max} \end{cases} \end{aligned} \tag{16}$$

Decision variables u_n and v_n represent sets of the two-dimensional location and speed of UAV base station at all time slots, while K and N represent the total number of moving ground users and communication time slots. ΔT is the interval of each time slot and P_0 counts for typical transmission power of UAV; therefore, $\sum_n^N \sum_i E_{i,n}^C$ represents energy consumption of communication, while $\sum_n^N E_n^F$ is flight energy consumption. u_n stands for location of UAV at time slot n , and a_n indicates the direction of UAV.

3.3. Transmission Power Subtask Optimization

When the location and bandwidth sub-optimization blocks are fixed, the sup-optimization problem of UAV transmission power consumption can be built by the same format. As transmission power multiplying P_{ug} term, it can influence the objective function:

$$\begin{aligned} \text{Objective} &= \sum R_i \\ &= \sum B * \log_2 \left(1 + \frac{P_{ug}(u_i, e_j)}{\sigma^2} \right) \\ &= \sum B * \log_2 \left(1 + \frac{P_u G(d_j)}{(k_0 d_{ij})^n (p_{LoS} \phi_{LoS} + p_{NLoS} \phi_{NLoS})} \cdot \frac{1}{\sigma^2} \right). \end{aligned} \tag{17}$$

At every time slot, the objective function R_i corresponding to ground user i can be calculated based on transmission power, effective communication bandwidth distributed to user i , and current UAV location. In the power optimization block, the initial bandwidth allocation and UAV moving strategy and fixed as follows, which are simply compliant with velocity and bandwidth constraints:

$$\begin{aligned} B_i &= B/K. \\ u_n &= u_{n-1} + [v_0 \cdot \cos a_0, v_0 \cdot \sin a_0]. \end{aligned} \tag{18}$$

When other environmental conditions are static, communication efficiency can grow with transmission power. Thus, to optimize UAV transmission power $P_{u,n}$ at time slot n , necessary constraints need to be specified. Relative constraints focus on the upper range of transmission power and total energy consumption, and the sub-optimization problem is shown as follows:

$$\begin{aligned} & \max_{P_{u,n}} \sum_n^N \sum_i^K R_{i,n} \\ & \text{s.t.} \quad \begin{cases} 0 \leq P_{u,n} \leq P_{max} \\ \sum_n^N P_{u,n} \Delta T + E_n^F \leq E_{max} \end{cases} \end{aligned} \tag{19}$$

Single decision variable $P_{u,n}$ denotes the transmission power of UAV at time slot n , while the upper bound is set as P_{max} . Energy constraints are consistent with that in the location optimization block discussed above, limiting transmission power from selecting the maximum at all times.

3.4. Communication Bandwidth Allocation Subtask Optimization

The third sub-optimization block pertains to the allocation of bandwidth, which encompasses a decision variable dimension of significant magnitude.

$$\begin{aligned} \text{Objective} &= \sum R_i \\ &= \sum B_i * \log_2(1 + \text{SINR}). \end{aligned} \quad (20)$$

To ensure optimal communication efficiency for all users, it is imperative to guarantee that the allocated bandwidth does not fall below the minimal threshold required for the successful transmission of communication data, resulting in constraint on R_i . An equal constraint is also given in this sub-block, as the sum of allocated bandwidths needs to be no more than B , but with no waste.

$$\begin{aligned} \max_{B_i} & \sum_n^N \sum_i^K R_{i,n} \\ \text{s.t.} & \begin{cases} R_{min} \leq R_i \\ \sum_i^K B_i = B. \end{cases} \end{aligned} \quad (21)$$

Decision variable B_i refers to bandwidth resource allocated to user i at a certain time slot. After these three sub-optimization tasks iterate and eventually converge, a multi-stage planning scheme can be proposed as follows, with sets of decision variables including U , B , and P , regarding UAV location, bandwidth allocation, and power control strategy, respectively. After all, our designed multi-subtask algorithm is established, with three sub-block problem consisting the total optimization function.

$$\begin{aligned} \max_{UBP} & \sum_n^N \sum_i^K R_{i,n} \\ \text{s.t.} & \begin{cases} 0 \leq P_u \leq P_{max} \\ \sum_i^C E_{i,n} + E_n^F \leq E_{max} \\ \sum B_{i,n} \leq B_i \\ v_n \leq v_{max} \\ R_{min} \leq R_i \end{cases} \end{aligned} \quad (22)$$

4. Numerical Results and Analysis

In this section, we validate the efficiency and robustness of the proposed optimization method under different UAV heights and environments. The optimized planned trajectory and time sequence of communication resources are also demonstrated, under our assumptions introduced in the model establishment, and trajectory prediction of moving ground users. Figure 5 demonstrates path planning for several scenarios.

To train UAV planning, the trajectory of moving ground users needs specification at first. With the CA model mentioned above, we have obtained the predicted data of ground users' location along the time sequence successfully.

For a simple demonstration and test, the number of ground users is set as 10, and the range of earthquake-stricken area is rectangular with length = 100 m and width = 50 m, with several obstacles scattered in, resembling residential buildings. The typical speed of a moving user in adequate wide space is 5 m/s, with evacuation time discretized into a time series with an interval of 1 s. All the residents have already left architecture at the first second, with random locations in the valid areas. As time passes, all users move in the shortest path directed to escape. In this simulation, the evacuation is completed in 80 s, thus we obtain the predicted trajectory of moving ground users. The software interface of the simulation is shown in Figure 6.

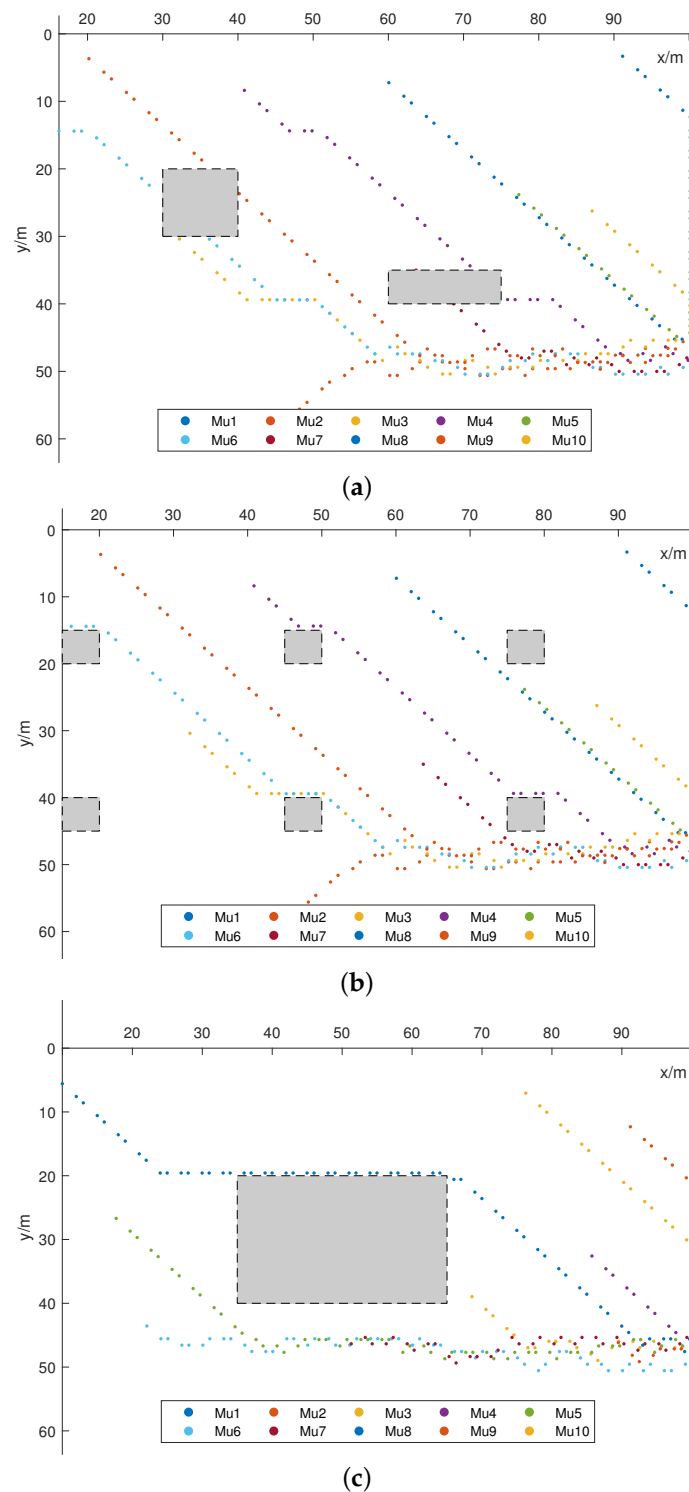


Figure 5. Trajectory of ground users predicted by CA model. The moving trajectories of considered users are depicted using scatter plots in different colors, showing that they effectively avoided obstacles and found the shortest possible paths to the exit, in different tested scenarios. (a) Predicted trajectory of moving users with 2 obstacles of different sizes. (b) The predicted trajectory of moving users with 6 scattered obstacles. (c) Predicted trajectory of moving users with 1 centered obstacle.

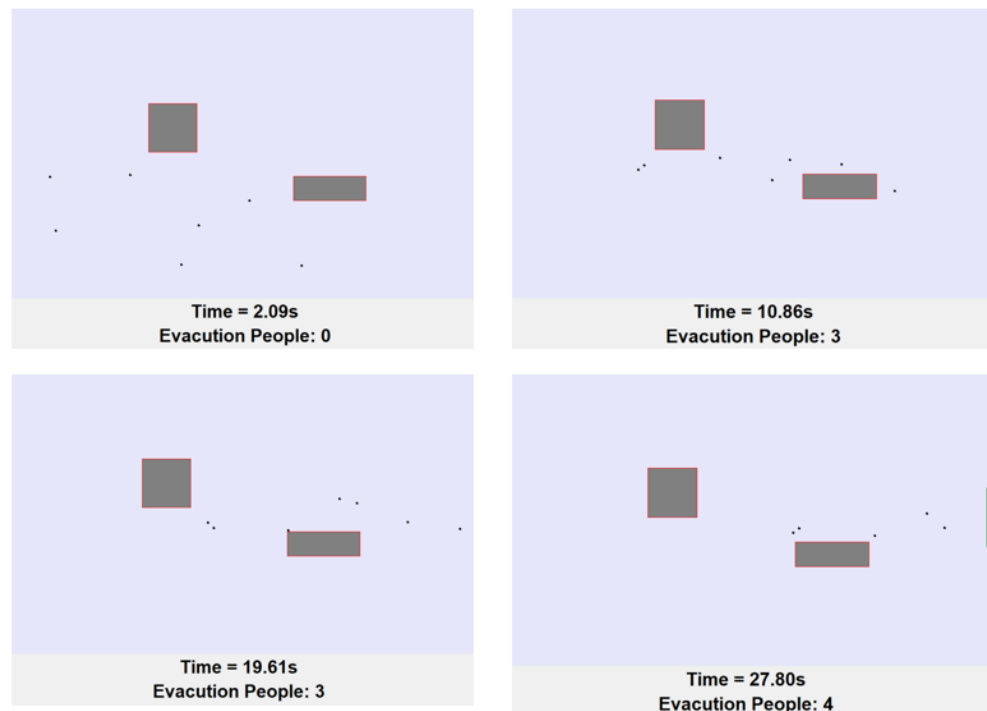


Figure 6. Software Illustration of ground users' moving trajectory simulation. As time passes, the number of evacuation people updates and provides a real-time demonstration of user evacuation movement based on CA simulation.

As the simulated results demonstrate, the trajectory of users can be predicated and the data can be applied to train ISATR later. We have generated different user trajectories to evaluate the adaptability of our proposed method, with scenarios varied in user distribution, obstacles, and exits.

4.1. Evaluation of UAV Trajectory planning

Based on the environmental information and user trajectories determined above, trajectory planning for the UAV base station has been achieved through the iterative optimization algorithm for trajectory sub-block problem, with parameters in the other two sub-block problems fixed.

As shown in Figure 7, the proposed trajectory planning method achieves the fastest convergence. Compared to several path planning methods including A* and genetic algorithm (GA), our optimized path planning strategy performs best in the discussed environment.

Visualization of the planned UAV trajectory is given in Figure 8, with trajectories of 10 moving users also displayed.

In each sub-graph, we release the aerial base station from different initial points and test the algorithm with different user distributions, finding that it maintains stability and moves synchronously with the trajectories of users toward the exit. In Figure 8a,b, there are two different-sized obstacle buildings in the environment, with the exit located at the center-right of the map. The UAVs are released from different initial positions, demonstrating their adaptability to different initial release positions. In Figure 8c,d, the exit is set at the bottom-right corner of the map. The scenarios with six dispersed obstacles and one central obstacle in the map are tested, thus validating the effectiveness of the algorithm in different scenarios.

Meanwhile, the number of inflection points on the convergence curve matches the number of users specified in the simulation, lending reasonable support to the optimization's correctness. Therefore, the effectiveness and robustness of the proposed trajectory planning algorithm are validated.

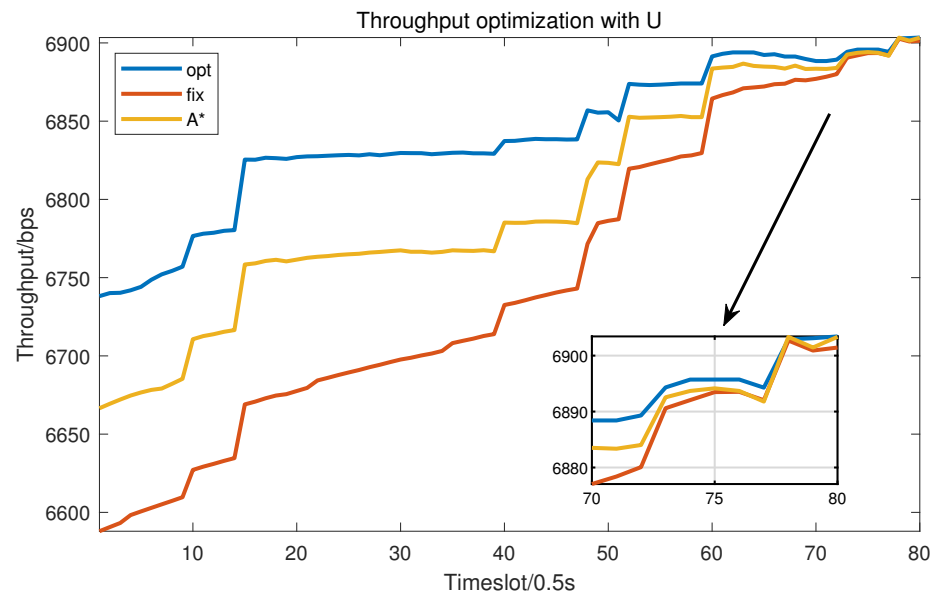


Figure 7. Throughput optimized with UAV trajectory in different methods. It can be found that our ISATR opt method outperforms the traditional A* algorithm and the algorithm with fixed UAV trajectory.

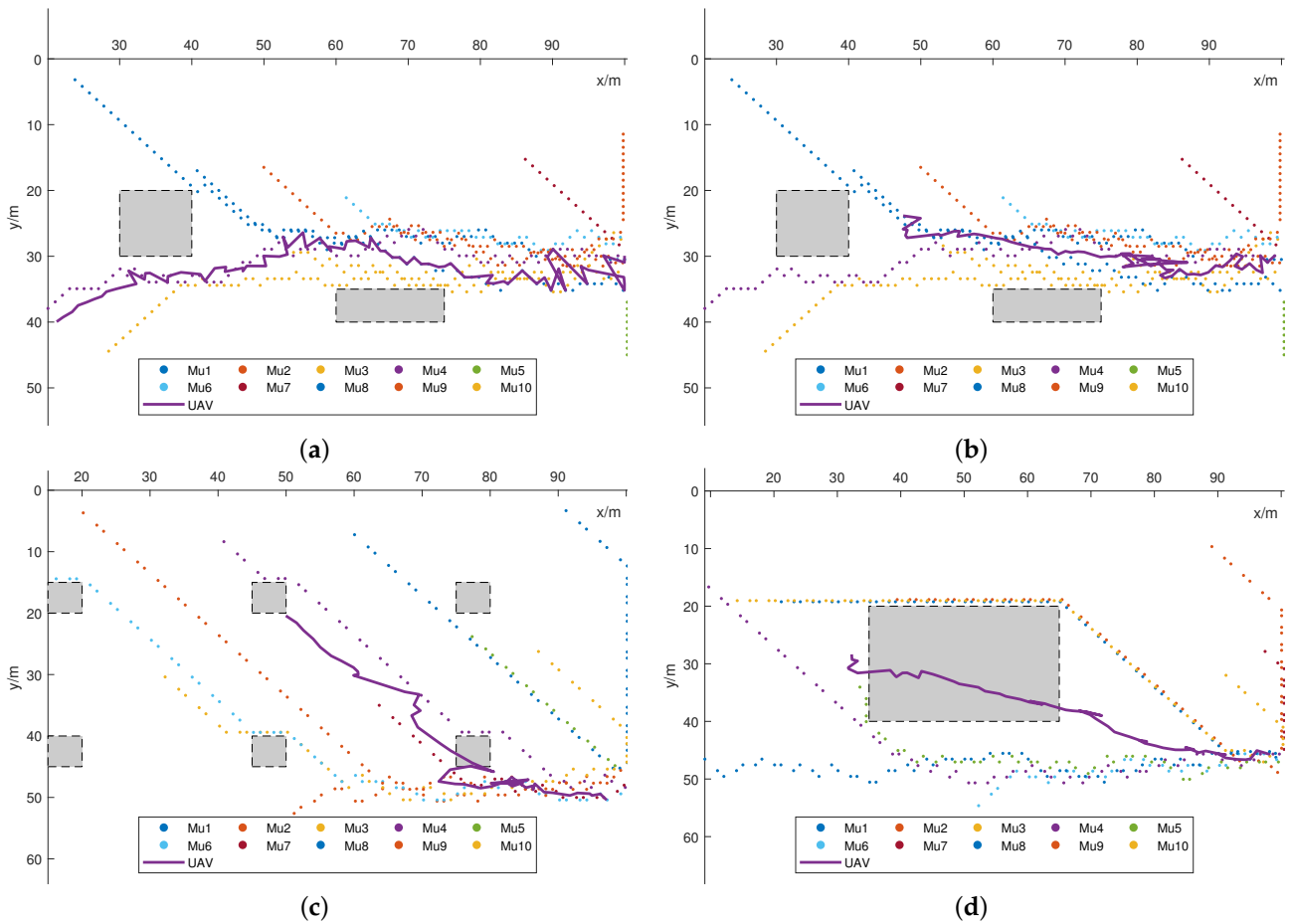


Figure 8. Trajectory planning illustration. Different initial positions for UAV trajectory optimization via ISATR are tested to verify the effectiveness and robustness of our algorithm. It can be seen that the trajectory of UAV is always consistent with users. (a) ISATR opted path 1. (b) ISATR opted path 2. (c) ISATR opted path 3. (d) ISATR opted path 4.

4.2. Evaluation of Resource Allocation

Besides path planning of the UAV base station, communication resource allocation also matters. Transmission power and bandwidth allocation for all ground users at different time slots are derived via our designed optimization algorithm.

It can be seen in Figures 9 and 10 that as time passes, the bandwidth allocation varies as the power of the UAV increases because the number of users in the valid area decreases. It is worth noting that there are 10 significant changes in P of the UAV base station, which is equal to the number of moving ground users, making it consistent with the logic of algorithm optimization.

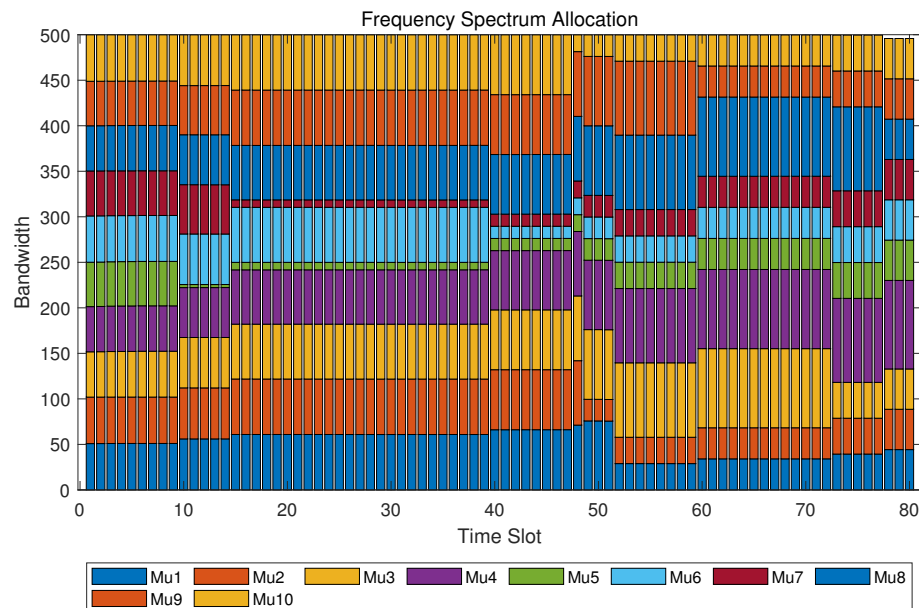


Figure 9. Bandwidth allocation illustration. Bandwidth allocation scheduling is influenced by the positions of UAV and users, as well as the power of UAV, also adhering to the minimum throughput constraint.

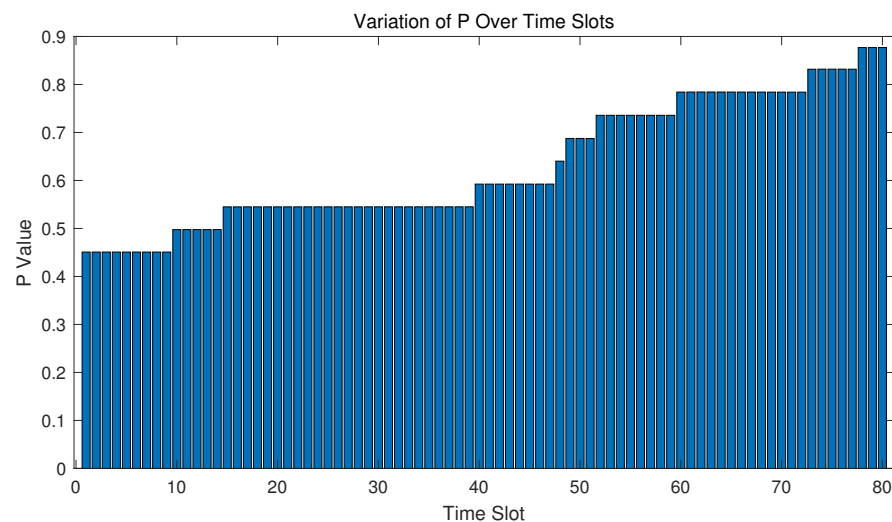


Figure 10. Power control illustration. UAV transmission power control is influenced by the positions of UAV and users, as well as the current bandwidth allocation, also adhering to the minimum throughput constraint.

4.3. Evaluation of Trajectory and Resource Joint Optimization

With UAV location, bandwidth allocation, and transmission power all optimized, total throughput in the communication system has an obvious increase, as illustrated in Figure 11.

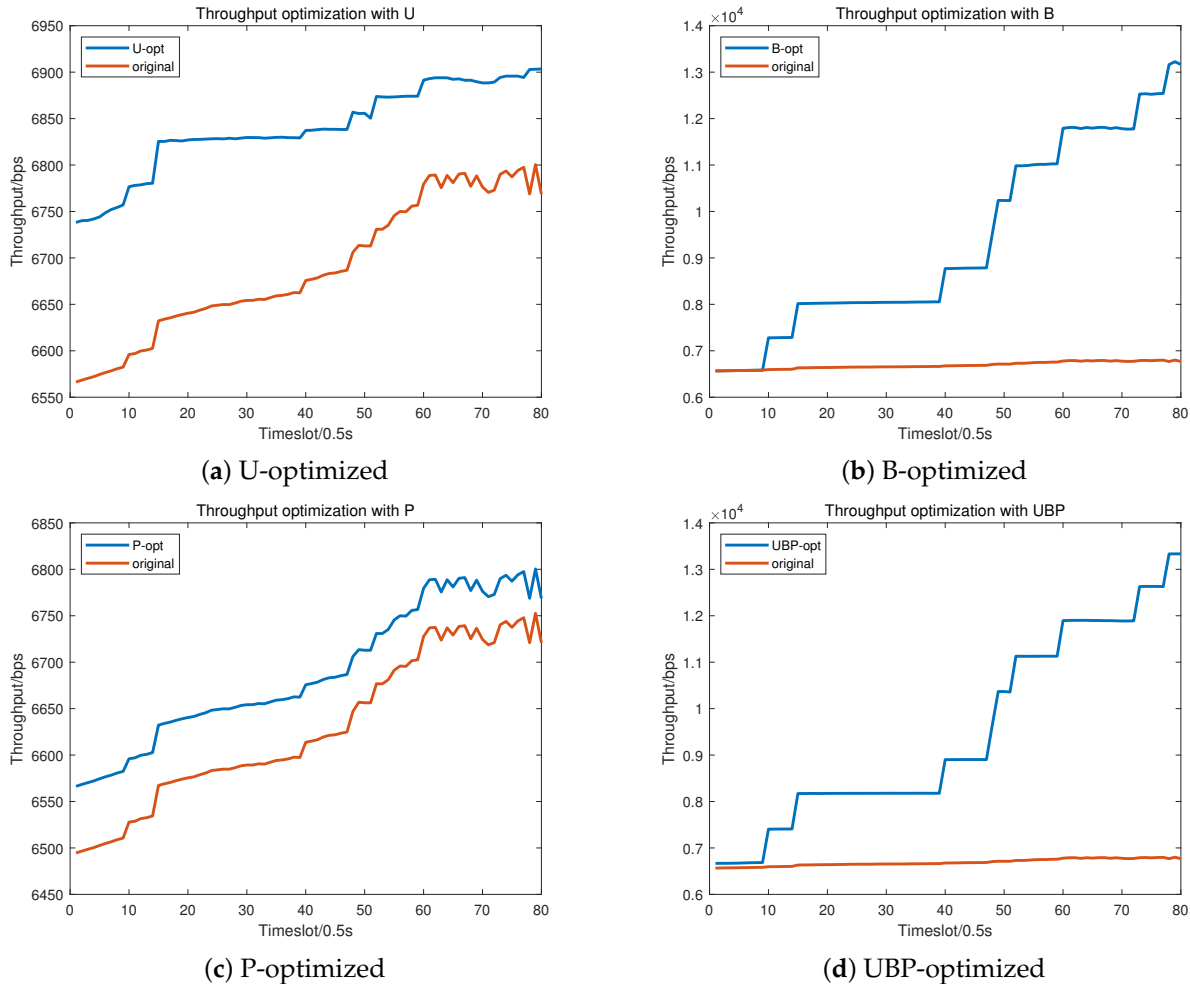
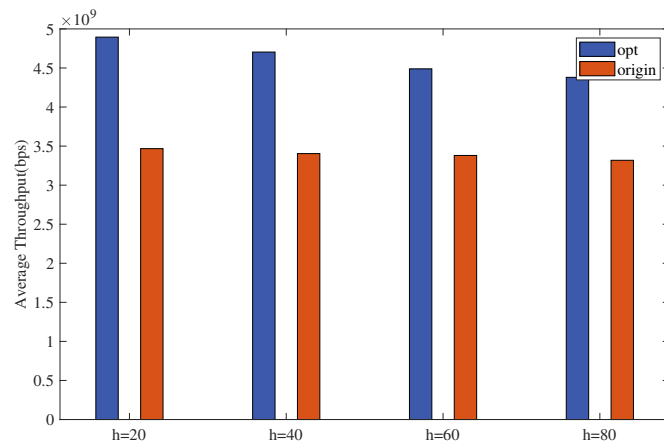


Figure 11. Throughput optimized with different decision variables. (a) Throughput with U (UAV location) optimized. (b) Throughput with B (bandwidth allocation) optimized. (c) Throughput with P (power of UAV) optimized. (d) Throughput with U, B, and P optimized.

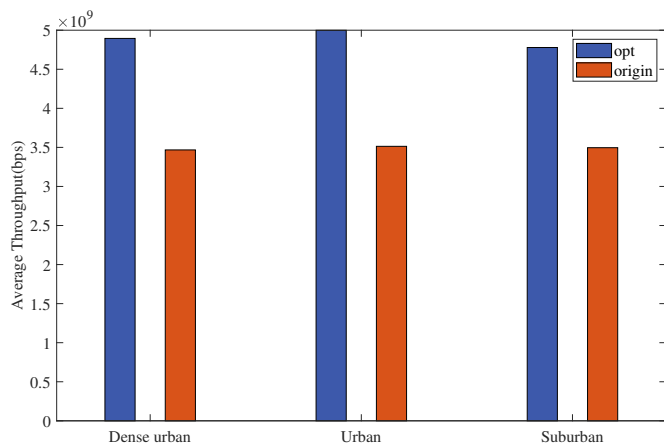
The optimization of the three components, U, B, and P, can be seen to have all contributed to the improvement in throughput, with the combined optimization demonstrating better performance compared to the contrast algorithms. Among them, the optimization of B presents a step-like pattern, attributed to the consideration of the issue where ground users leaving the valid area are not involved in allocation in this algorithm. It can be observed that the number of steps is consistent with the total number of users.

Moreover, we select the average total throughput observed over the time sequence of simulation as the evaluation metric and compare our method with several alternative strategies, experimenting with various sets of environmental information. At different heights, the UAV adjusts the routing plan and resource allocation strategy according to the optimization functions, maintaining a stable optimization effect, as shown in Figure 12.

In Figure 13, the throughput optimization achieved by various methods is depicted, highlighting the superior performance of our ISATR method compared to the others. The compared methods include A*, GA, and fixed algorithm, in which “fixed” refers to the non-optimized case.



(a)



(b)

Figure 12. Average total throughput illustration in typical environments. (a) Throughput optimized at different heights. (b) Throughput optimized in different environments. Compared to the non-optimized value, the ISATR method has an increase of 42%.

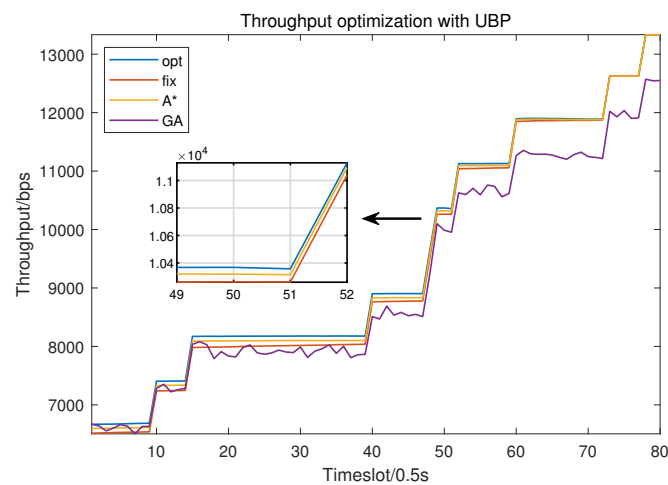


Figure 13. Throughput optimization with different methods. Throughput with location, bandwidth allocation, and power control optimized via different algorithms, including the proposed opt method (ISATR), GA method, A* method, and fixed case. ISATR outperforms the others.

5. Discussion

In the above sections, we have introduced an iterative algorithm ISATR to tackle the joint optimization problem of UAV-assisted communication, involving trajectory planning, power control, and bandwidth allocation. This proposed algorithm is dedicated to providing the pre-planning scheme of a UAV as a temporary base station in an emergency scenario. It can serve as a necessary baseline in case of emergencies, benefiting from its high accuracy.

Therefore, it is necessary to combine ISATR with other real-time algorithms, such as deep reinforcement learning (DRL), for practical implications. The main difference between ISATR and DRL is that their application scenarios are complementary. The former is applied to pre-planning which requires high accuracy, while the latter is applied to dynamic planning that requires real-time response. DRL-based UAV planning algorithm will be studied in future work to provide a dynamic response.

Physical limitations of UAVs are also essential in UAV-assisted systems. One notable drawback lies in the current weight and complexity of UAV systems, which can pose challenges in rapid deployment, particularly in emergency scenarios where swift action is imperative. To address these limitations, future research could focus on advancing lightweight UAV designs and streamlined deployment mechanisms. Integration of advanced materials and miniaturized components could significantly reduce the weight and size of UAVs, facilitating quick and agile deployment even in constrained environments.

6. Conclusions

This paper discusses a UAV-assisted communication scenario in an earthquake-stricken cellular cell. As the ground base station is devastated and blocked, a UAV is dispatched as a temporary aerial base station. An ISATR (iterative scheduling algorithm of trajectory and resource) is constructed to solve optimization questions to enhance the UAV's communication efficiency. A trajectory prediction model is derived via cellular automata and provides location data of ground users in evacuation for the UAV's decision. Path planning and resource allocation including bandwidth distribution and transmission power control are involved in the decision space, and the total throughput of A2G channels is considered as the objective function in optimization. With our designed multi-stage subtask iteration optimization algorithm, the total throughput is enhanced. Compared to the traditional optimization method GA and path planning method A*, our method has an advantage in higher optimization performance. Finally, we have an enhancement of approximately 40% total throughput tested in several typical environments, compared to non-optimized cases, which indicates that the proposed method can serve as an effective algorithm for pre-planning emergency UAV scheduling tasks.

Author Contributions: Conceptualization, Z.Z. and Y.L.; methodology, Z.Z., Y.W., and Y.L.; software and validation, Z.Z. and X.Z.; formal analysis, H.Z.; investigation, Z.Z. and W.D.; resources, Y.W.; data curation, Y.L.; writing—original draft preparation, Z.Z. and X.Z.; writing—review and editing, Y.L. and Y.W.; visualization, Z.Z. and H.Z.; supervision, W.D.; project administration, W.D.; funding acquisition, W.D. All authors have read and agreed to the published version of the manuscript.

Funding: This research was funded by National Natural Science Foundation of China (U20B2042).

Data Availability Statement: The data used to support this study have not been made available.

Conflicts of Interest: The authors declare no conflicts of interest.

References

1. Zeng, Y.; Zhang, R.; Lim, T.J. Wireless communications with unmanned aerial vehicles: Opportunities and challenges. *IEEE Commun. Mag.* **2016**, *54*, 36–42. [[CrossRef](#)]
2. Kim, H.; Ben-Othman, J. A Collision-Free Surveillance System Using Smart UAVs in Multi Domain IoT. *IEEE Commun. Lett.* **2018**, *22*, 2587–2590. [[CrossRef](#)]

3. Hasan, K.M.; Suhaili, W.S.; Shah Newaz, S.H.; Ahsan, M.S. Development of an Aircraft Type Portable Autonomous Drone for Agricultural Applications. In Proceedings of the 2020 International Conference on Computer Science and Its Application in Agriculture (ICOSICA), Bogor, Indonesia, 16–17 September 2020; pp. 1–5. [\[CrossRef\]](#)
4. Alsawy, A.; Hicks, A.; Moss, D.; Mckeever, S. An Image Processing Based Classifier to Support Safe Dropping for Delivery-by-Drone. In Proceedings of the 2022 IEEE 5th International Conference on Image Processing Applications and Systems (IPAS), Genova, Italy, 5–7 December 2022; Volume 5, pp. 1–5. [\[CrossRef\]](#)
5. Alrayes, F.S.; Alzahrani, J.S.; Alissa, K.A.; Alharbi, A.; Alshahrani, H.; Elfaki, M.A.; Yafoz, A.; Mohamed, A.; Hilal, A.M. Dwarf Mongoose Optimization-Based Secure Clustering with Routing Technique in Internet of Drones. *Drones* **2022**, *6*, 247. [\[CrossRef\]](#)
6. Samir, M.; Sharafeddine, S.; Assi, C.M.; Nguyen, T.M.; Ghayeb, A. UAV Trajectory Planning for Data Collection from Time-Constrained IoT Devices. *IEEE Trans. Wirel. Commun.* **2020**, *19*, 34–46. [\[CrossRef\]](#)
7. Huang, Z.; Chen, C.; Pan, M. Multiobjective UAV Path Planning for Emergency Information Collection and Transmission. *IEEE Internet Things J.* **2020**, *7*, 6993–7009. [\[CrossRef\]](#)
8. Xu, J.; Ota, K.; Dong, M. Big Data on the Fly: UAV-Mounted Mobile Edge Computing for Disaster Management. *IEEE Trans. Netw. Sci. Eng.* **2020**, *7*, 2620–2630. [\[CrossRef\]](#)
9. Jeong, S.; Simeone, O.; Kang, J. Mobile Edge Computing via a UAV-Mounted Cloudlet: Optimization of Bit Allocation and Path Planning. *IEEE Trans. Veh. Technol.* **2018**, *67*, 2049–2063. [\[CrossRef\]](#)
10. Asad, M.; Aidaros, O.A.; Beg, R.; Dhahri, M.A.; Neyadi, S.A.; Hussein, M. Development of autonomous drone for gas sensing application. In Proceedings of the 2017 International Conference on Electrical and Computing Technologies and Applications (ICECTA), Ras Al Khaimah, United Arab Emirates, 21–23 November 2017; pp. 1–6. [\[CrossRef\]](#)
11. Wu, C.; Ju, B.; Wu, Y.; Lin, X.; Xiong, N.; Xu, G.; Li, H.; Liang, X. UAV Autonomous Target Search Based on Deep Reinforcement Learning in Complex Disaster Scene. *IEEE Access* **2019**, *7*, 117227–117245. [\[CrossRef\]](#)
12. Abeygunawardana, P.; Gamage, N.; De Alwis, L.; Ashan, S.; Nilanka, C.; Godamune, P. E-Medic—Autonomous Drone for Healthcare System. In Proceedings of the 2021 International Conference on Computing, Communication, and Intelligent Systems (ICCCIS), Greater Noida, India, 19–20 February 2021; pp. 994–999. [\[CrossRef\]](#)
13. Bitar, A.; Jamal, A.; Sultan, H.; Alkandari, N.; El-Abd, M. Medical Drones System for Amusement Parks. In Proceedings of the 2017 IEEE/ACS 14th International Conference on Computer Systems and Applications (AICCSA), Hammamet, Tunisia, 30 October–3 November 2017; pp. 19–20. ISSN: 2161-5330. [\[CrossRef\]](#)
14. Besada, J.A.; Bernardos, A.M.; Bergesio, L.; Vaquero, D.; Campaña, I.; Casar, J.R. Drones-as-a-service: A management architecture to provide mission planning, resource brokerage and operation support for fleets of drones. In Proceedings of the 2019 IEEE International Conference on Pervasive Computing and Communications Workshops (PerCom Workshops), Kyoto, Japan, 11–15 March 2019; pp. 931–936. [\[CrossRef\]](#)
15. Yan, C.; Fu, L.; Zhang, J.; Wang, J. A Comprehensive Survey on UAV Communication Channel Modeling. *IEEE Access* **2019**, *7*, 107769–107792. [\[CrossRef\]](#)
16. Khawaja, W.; Guvenc, I.; Matolak, D.W.; Fiebig, U.C.; Schneckenburger, N. A Survey of Air-to-Ground Propagation Channel Modeling for Unmanned Aerial Vehicles. *IEEE Commun. Surv. Tutorials* **2019**, *21*, 2361–2391. [\[CrossRef\]](#)
17. Alsamhi, S.H.; Shvetsov, A.V.; Shvetsova, S.V.; Hawbani, A.; Guizani, M.; Alhartomi, M.A.; Ma, O. Blockchain-Empowered Security and Energy Efficiency of Drone Swarm Consensus for Environment Exploration. *IEEE Trans. Green Commun. Netw.* **2023**, *7*, 328–338. [\[CrossRef\]](#)
18. Srivastava, K.; Pandey, P.C.; Sharma, J.K. An Approach for Route Optimization in Applications of Precision Agriculture Using UAVs. *Drones* **2020**, *4*, 58. [\[CrossRef\]](#)
19. Luan, Q.; Cui, H.; Zhang, L.; Lv, Z. A Hierarchical Hybrid Subtask Scheduling Algorithm in UAV-Assisted MEC Emergency Network. *IEEE Internet Things J.* **2022**, *9*, 12737–12753. [\[CrossRef\]](#)
20. Cabreira, T.M.; Brisolara, L.B.; Ferreira, P.R., Jr. Survey on Coverage Path Planning with Unmanned Aerial Vehicles. *Drones* **2019**, *3*, 4. [\[CrossRef\]](#)
21. Al-Hourani, A.; Kandeepan, S.; Jamalipour, A. Modeling air-to-ground path loss for low altitude platforms in urban environments. In Proceedings of the 2014 IEEE Global Communications Conference, Austin, TX, USA, 8–12 December 2014; pp. 2898–2904. ISSN: 1930-529X. [\[CrossRef\]](#)
22. Lyu, Y.; Wang, W.; Sun, Y.; Yue, H.; Chai, J. Low-Altitude UAV Air-to-Ground Multilink Channel Modeling and Analysis at 2.4 and 5.9 GHz. *IEEE Antennas Wirel. Propag. Lett.* **2023**, *22*, 2135–2139. [\[CrossRef\]](#)
23. Goddemeier, N.; Daniel, K.; Wietfeld, C. Role-Based Connectivity Management with Realistic Air-to-Ground Channels for Cooperative UAVs. *IEEE J. Sel. Areas Commun.* **2012**, *30*, 951–963. [\[CrossRef\]](#)
24. Ge, C.; Zhai, D.; Jiang, Y.; Zhang, R.; Yang, X.; Li, B.; Tang, X. Pathloss and Airframe Shadowing Loss of Air-to-Ground UAV Channel in the Airport Area at UHF- and L-Band. *IEEE Trans. Veh. Technol.* **2023**, *72*, 8094–8098. [\[CrossRef\]](#)
25. Li, H.; Ding, L.; Wang, Y.; Wang, Z. Air-to-Ground Channel Modeling and Performance Analysis for Cellular-Connected UAV Swarm. *IEEE Commun. Lett.* **2023**, *27*, 2172–2176. [\[CrossRef\]](#)
26. Wang, S.; Lim, T.H.; Choo, H. Path Loss Analysis Considering Atmospheric Refractivity and Precipitation for Air-to-Ground Radar. *IEEE Antennas Wirel. Propag. Lett.* **2021**, *20*, 1968–1972. [\[CrossRef\]](#)
27. Cui, Z.; Guan, K.; Oestges, C.; Briso-Rodríguez, C.; Ai, B.; Zhong, Z. Cluster-Based Characterization and Modeling for UAV Air-to-Ground Time-Varying Channels. *IEEE Trans. Veh. Technol.* **2022**, *71*, 6872–6883. [\[CrossRef\]](#)

28. Wan, Y.; Zhong, Y.; Ma, A.; Zhang, L. An Accurate UAV 3-D Path Planning Method for Disaster Emergency Response Based on an Improved Multiobjective Swarm Intelligence Algorithm. *IEEE Trans. Cybern.* **2023**, *53*, 2658–2671. [[CrossRef](#)]
29. Wang, X.; Pan, J.; Yang, Q.; Kong, L.; Snašsel, V.; Chu, S. Modified Mayfly Algorithm for UAV Path Planning. *Drones* **2022**, *6*, 134. [[CrossRef](#)]
30. Zheng, L.; Tian, Y.; Wang, H.; Hong, C.; Li, B. Path Planning of Autonomous Mobile Robots Based on an Improved Slime Mould Algorithm. *Drones* **2023**, *7*, 257. [[CrossRef](#)]
31. Shen, Y.; Zhu, Y.; Kang, H.; Sun, X.; Chen, Q.; Wang, D. UAV Path Planning Based on Multi-Stage Constraint Optimization. *Drones* **2021**, *5*, 144. [[CrossRef](#)]
32. Wang, B.; Sun, Y.; Sun, Z.; Nguyen, L.D.; Duong, T.Q. UAV-Assisted Emergency Communications in Social IoT: A Dynamic Hypergraph Coloring Approach. *IEEE Internet Things J.* **2020**, *7*, 7663–7677. [[CrossRef](#)]
33. Prasad, N.L.; Ramkumar, B. 3-D Deployment and Trajectory Planning for Relay Based UAV Assisted Cooperative Communication for Emergency Scenarios Using Dijkstra’s Algorithm. *IEEE Trans. Veh. Technol.* **2023**, *72*, 5049–5063. [[CrossRef](#)]
34. Zhang, S.; Zeng, Y.; Zhang, R. Cellular-Enabled UAV Communication: A Connectivity-Constrained Trajectory Optimization Perspective. *IEEE Trans. Commun.* **2019**, *67*, 2580–2604. [[CrossRef](#)]
35. Jayaweera, H.; Hanoun, S. Path Planning of Unmanned Aerial Vehicles (UAVs) in Windy Environments. *Drones* **2022**, *6*, 101. [[CrossRef](#)]
36. Zhang, S.; Li, Y.; Ye, F.; Geng, X.; Zhou, Z.; Shi, T. A Hybrid Human-in-the-Loop Deep Reinforcement Learning Method for UAV Motion Planning for Long Trajectories with Unpredictable Obstacles. *Drones* **2023**, *7*, 311. [[CrossRef](#)]
37. Gubán, M.; Udvaros, J. A Path Planning Model with a Genetic Algorithm for Stock Inventory Using a Swarm of Drones. *Drones* **2022**, *6*, 364. [[CrossRef](#)]
38. Zhang, L.; Ma, X.; Zhuang, Z.; Xu, H.; Sharma, V.; Han, Z. Q-Learning Aided Intelligent Routing With Maximum Utility in Cognitive UAV Swarm for Emergency Communications. *IEEE Trans. Veh. Technol.* **2023**, *72*, 3707–3723. [[CrossRef](#)]
39. Zhang, T.; Lei, J.; Liu, Y.; Feng, C.; Nallanathan, A. Trajectory Optimization for UAV Emergency Communication With Limited User Equipment Energy: A Safe-DQN Approach. *IEEE Trans. Green Commun. Netw.* **2021**, *5*, 1236–1247. [[CrossRef](#)]
40. Qie, H.; Shi, D.; Shen, T.; Xu, X.; Li, Y.; Wang, L. Joint Optimization of Multi-UAV Target Assignment and Path Planning Based on Multi-Agent Reinforcement Learning. *IEEE Access* **2019**, *7*, 146264–146272. [[CrossRef](#)]
41. Wang, F.; Xu, X.; Chen, M.; Nzige, J.; Chong, F. Simulation Research on Fire Evacuation of Large Public Buildings Based on Building Information Modeling. *Complex Syst. Model. Simul.* **2021**, *1*, 122–130. [[CrossRef](#)]
42. Hou, Z.; Sun, Y.; Cai, M. 3D Visualization of Forest Fire Spread Model Based on Cellular Automata. In Proceedings of the 2023 8th International Conference on Computer and Communication Systems (ICCCS), Guangzhou, China, 21–23 April 2023; pp. 880–883. [[CrossRef](#)]
43. Ye, Z.; Yin, Y.; Zong, X.; Wang, M. An Optimization Model for Evacuation Based on Cellular Automata and Ant Colony Algorithm. In Proceedings of the 2014 Seventh International Symposium on Computational Intelligence and Design, Hangzhou, China, 13–14 December 2014; Volume 1, pp. 7–10. [[CrossRef](#)]

Disclaimer/Publisher’s Note: The statements, opinions and data contained in all publications are solely those of the individual author(s) and contributor(s) and not of MDPI and/or the editor(s). MDPI and/or the editor(s) disclaim responsibility for any injury to people or property resulting from any ideas, methods, instructions or products referred to in the content.